Interaction of particles with matter, detectors, accelerators

Panos Christakoglou[1,2]

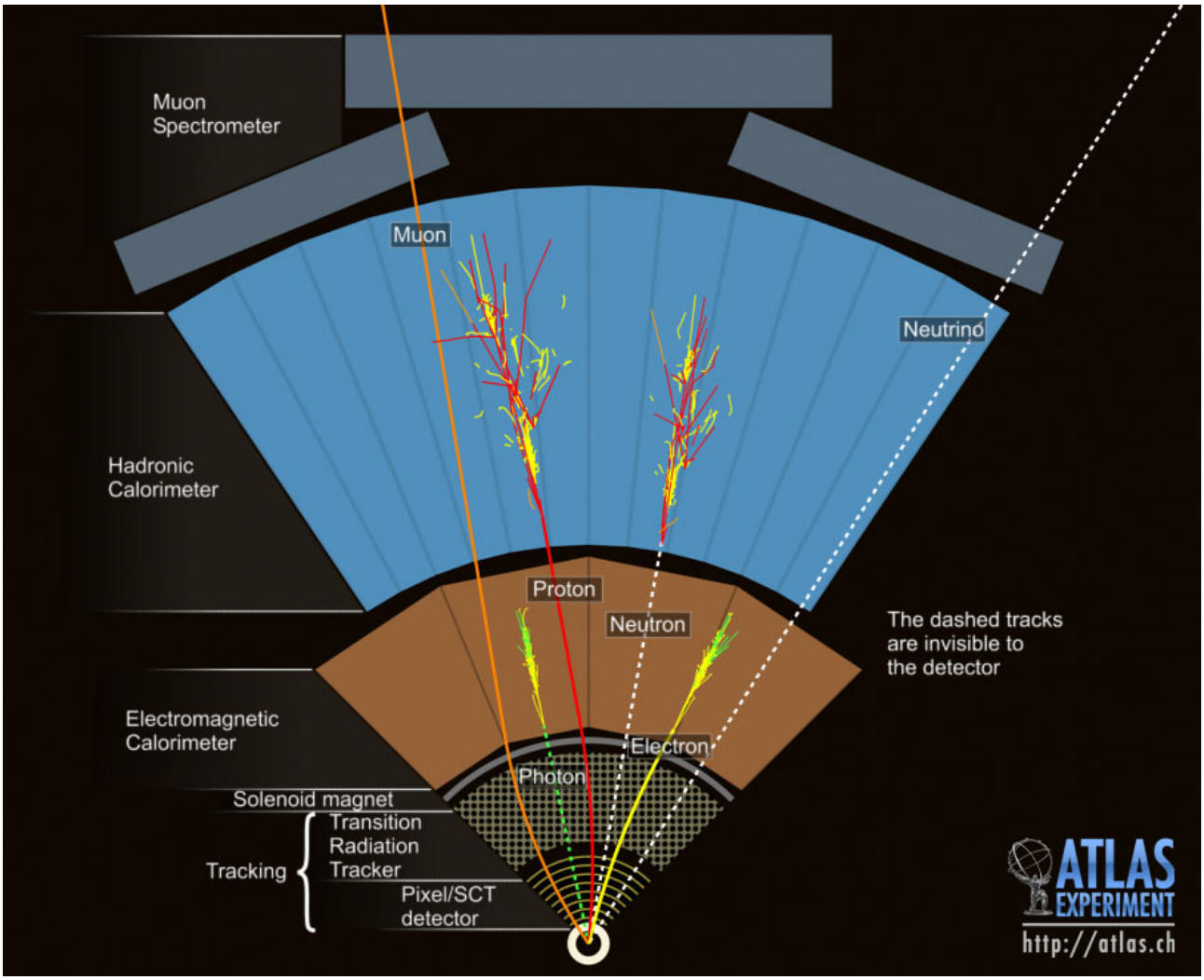

[1] P.Christakoglou@uu.nl - Utrecht University, Leonard S. Ornsteinlaboratorium Princetonplein 1, 3584CC Utrecht, The Netherlands
[2] Panos.Christakoglou@nikhef.nl - Nikhef, Science Park 105, 1098XG Amsterdam, The Netherlands

Contents

Chapter 1

Interactions of particles with matter and introduction to detection techniques

Particle physics experiments are designed to detect and identify particles produced in high-energy collisions. Of these particles, only the electrons, protons, photons and the notoriously hard to detect neutrinos are stable. Unstable particles travel a certain distance of the order of $\gamma v\tau$ before decaying, where here τ is the mean lifetime in the rest frame of the particle and $\gamma = (1 - v^2/c^2)^{-1/2}$ is the Lorentz factor that accounts for the relativistic time dilation.

Relativistic particles with a lifetime greater than around 10^{-10} s will propagate over several meters when produced in high-energy particle collisions and thus can be detected directly. The long-lived particles include the muon ($\mu^{\pm}$), the charged pions ($\pi^{\pm}$) and charged kaons ($K^{\pm}$). Short-lived particles with lifetimes less than about 10^{-10} s will typically decay before they travel a significant distance from the point of production and only their decay products can be thus detected.

All these categories of particles, both stable and unstable, form the environment inside of which modern particle physics experiments operate. The goal of these experiments is to reconstruct and identify these particles. The techniques used to both detect and identify them differs and depends on the nature of their interaction with matter. Generally speaking, particle interactions can be divided into three categories:

- the interaction with charged particles,
- the electromagnetic interactions of electrons and photons,
- the strong interactions of charged and neutral hadrons.

1.1 Interaction of charged particles with matter

When a relativistic charged particle passes through a medium it interacts electromagnetically with the atomic electrons and loses energy through ionisation of the atoms. For a singly charged particle with velocity $v = \beta c$ traversing a medium with atomic number Z and number density n, the ionisation energy loss per unit length traversed is given by the Bethe-Bloch equation, according to

$$\frac{dE}{dx} \approx -4\pi\hbar^2 c^2 \alpha^2 \frac{nZ}{m_e v^2}\left[ln\Big(\frac{2\beta^2\gamma^2 c^2 m_e}{I_e}\Big) - \beta^2\right] \tag{1.1.1}$$

In this equation I_e is the effective ionisation potential of the material averaged over all atomic electrons, which is very approximately given by $I_e \approx 10Z$ eV. For a particular medium, the rate of the ionisation energy loss of a charged particle is a function of its velocity. Owing to its $1/v^2$ term in the Bethe-Bloch equation, dE/dx is greatest for low-velocity particles. Modern particle physics is mainly interested though in highly relativistic particles with $v \approx c$. In this case, for a given medium, dE/dx depends logarithmically on $(\beta\gamma)^2$ where

$$\beta\gamma = \frac{v/c}{\sqrt{1-(v/c)^2}} = \frac{p}{mc},$$

resulting into a slow relativistic rise of the rate of ionisation energy loss. The evolution of dE/dx as a function of $(\beta\gamma)$ is given in fig. 1.1. This also gives the stopping power. As can be seen from ffig. 1.1, the $-\langle dE/dx\rangle$ defined in this way is about the same for most materials, decreasing slowly with Z. The rate of ionisation energy loss does not depend significantly on the material except through its density. This can be seen by expressing the number density of atoms as $n = \rho/(Am_u)$, where A is the atomic number and $m_u = 1.66 \times 10^{-27}$ kg is the unified atomic mass unit. The equation 1.1.1 can then be written as

$$\frac{1}{\rho}\frac{dE}{dx} \approx -\frac{4\pi\hbar^2c^2\alpha^2}{m_e v^2 m_u}\frac{Z}{A}\Big[ln\Big(\frac{2\beta^2\gamma^2c^2m_e}{I_e}\Big) - \beta^2\Big], \tag{1.1.2}$$

where the proportionality of the energy loss to Z/A becomes evident. Since nuclei contain approximately similar number of protons and neutrons, the ratio Z/A is roughly constant and thus the rate of energy loss by ionisation is proportional to density and does not depend strongly on the material. This can be better seen in fig. 1.1 which shows the ionisation energy loss as a function of $\beta\gamma$ for a singly charged particle in various materials. It is seen that particles with $\beta\gamma \approx 3$ which corresponds to the minimum ionisation energy loss curve are referred to as minimum ionising particles.

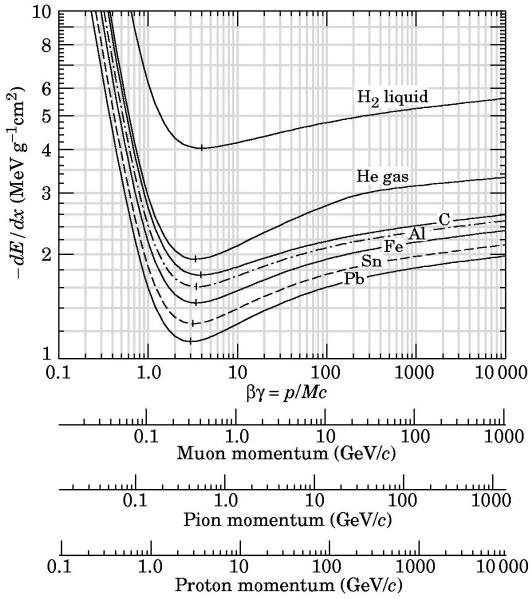

Fig. 1.1: Mean energy loss rate in liquid (bubble chamber) hydrogen, gaseous helium, carbon, aluminum, iron, tin, and lead. Radiative effects, relevant for muons and pions, are not included. These become significant for muons in iron for $\beta\gamma > 1000$ and at lower momenta for muons in higher-Z absorbers

All charged particles lose energy through ionisation of the medium in which the are propagating. Depending on the particle type, other energy-loss mechanisms maybe present. For muons with energies below 100 GeV, ionisation is the dominant energy loss as can be seen in fig. 1.2. That means that a muon travels significant distances even in dense materials like iron. As an example, a muon with energy of around 10 GeV loses approximately 13 MeV cm^{-1} in iron and thus will be able to travel for several meters. As a result, the muons produced in collisions of particles in modern particle accelerators are very penetrating particles, they usually traverse the entire detector and leave a trail of ionisation. This is the feature that can be exploited to identify muons experimentally.

1.1.1 Tracking detectors

The detection and measurement of momenta of charged particles is an essential aspect of every large particle physics experiment. Regardless of the medium, through which a charged particle travels, it leaves a trail of ionised atoms and

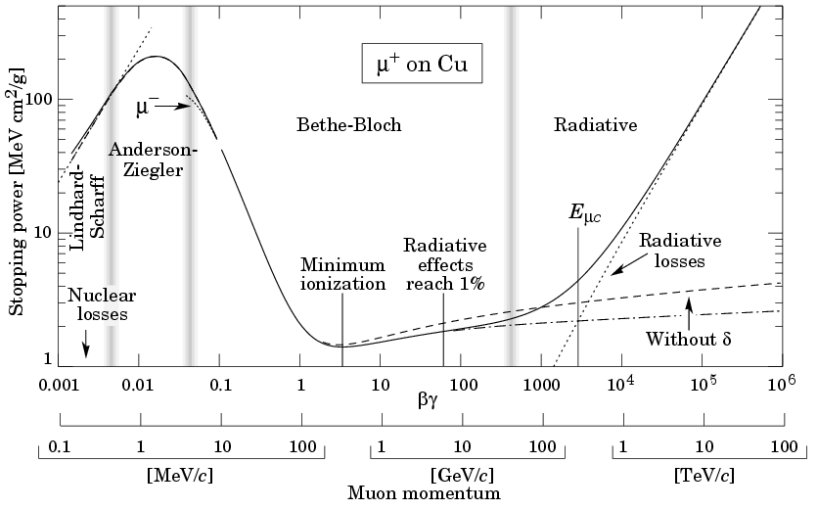

Fig. 1.2: Mass stopping power ($\approx -\langle dE/dx \rangle$) for positive muons in copper as a function of $\beta\gamma = p/Mc$ over nine orders of magnitude in momentum (12 orders of magnitude in kinetic energy).

liberated electrons. By detecting this ionisation it is possible to reconstruct the trajectory of a charged particle. There are two categories of tracking detectors used in modern experiments. Charged particles can be detected and their trajectories can be reconstructed in

- large gaseous detectors such as the TPC discussed before, where the liberated electrons are drifted in strong electric fields towards the sense wires where a signal is detected,
- detectors using semiconductor technology such as silicon pixels or strips.

1.1.1.1 Gaseous detectors

A detector that exploits this feature discussed above is the Time Projection Chamber (TPC). The TPC has been introduced in 1976 by D.R. Nygren. A TPC consists of a gas-filled detection volume in an electric field with a position-sensitive electron collection system. The design most commonly used is a cylindrical chamber with multi-wire proportional chambers (MWPC) as endplates. Along its length, the chamber is divided into halves by means of a central high-voltage electrode disc, which establishes an electric field between the centre and the end plates. Furthermore, a magnetic field is often applied along the length of the cylinder, parallel to the electric field, in order to minimise the diffusion of the electrons coming from the ionisation of the gas. On passing through the detector gas, a particle will produce primary ionisation along its track. The z coordinate (along the cylinder axis) is determined by measuring the drift time from the ionisation event to the MWPC at the end. This is done using the usual technique of a drift chamber. The MWPC at the end is arranged with the anode wires in the azimuthal direction, θ, which provides information on the radial coordinate, r. To obtain the azimuthal direction, each cathode plane is divided into strips along the radial direction.

The working principle of the TPC is sketched in fig. 1.3. A charged particle traversing the gas volume of the TPC will ionizes the atoms of the gas mixture (usually around 90% noble gas and 10% quencher gas) along its trajectory. A high electric field is applied between the endplates of the chamber. The released electrons drift in this field towards the anode. To be able to measure the position of the particle trajectory as accurately as possible, the electric field has to be very homogeneous. This can be achieved by a field cage, which usually consists of conducting rings around the cylinder. These rings divide the potential from the cathode stepwise down to the anode. Additionally, a high magnetic field parallel to the electric field is used to ”bend” the trajectory of the particle on a spiral track due to the Lorentz force. This gives the possibility to calculate the momentum of the particle from the knowledge of the curvature and the B-field.

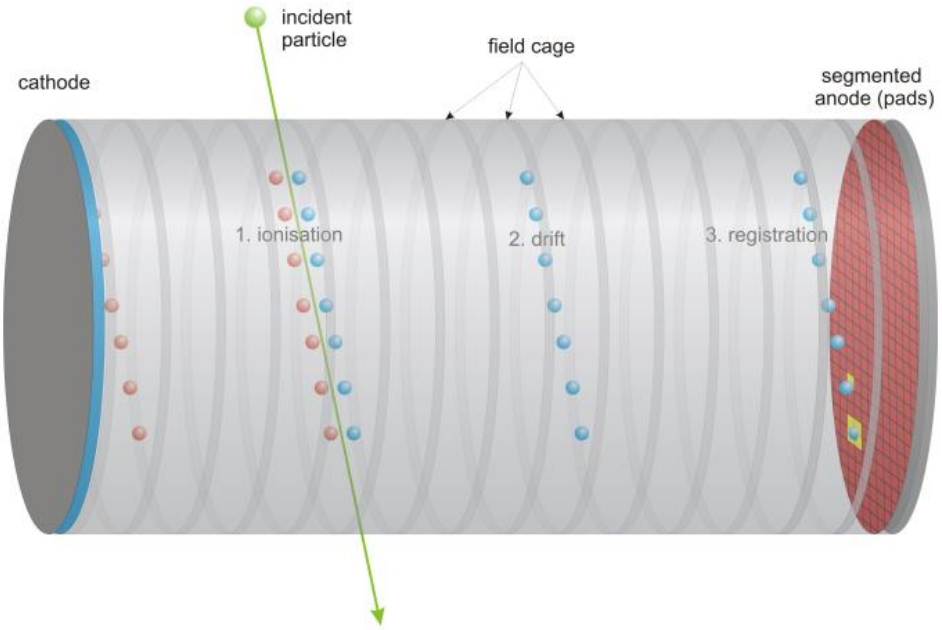

Fig. 1.3: The working principle of a Time Projection Chamber.

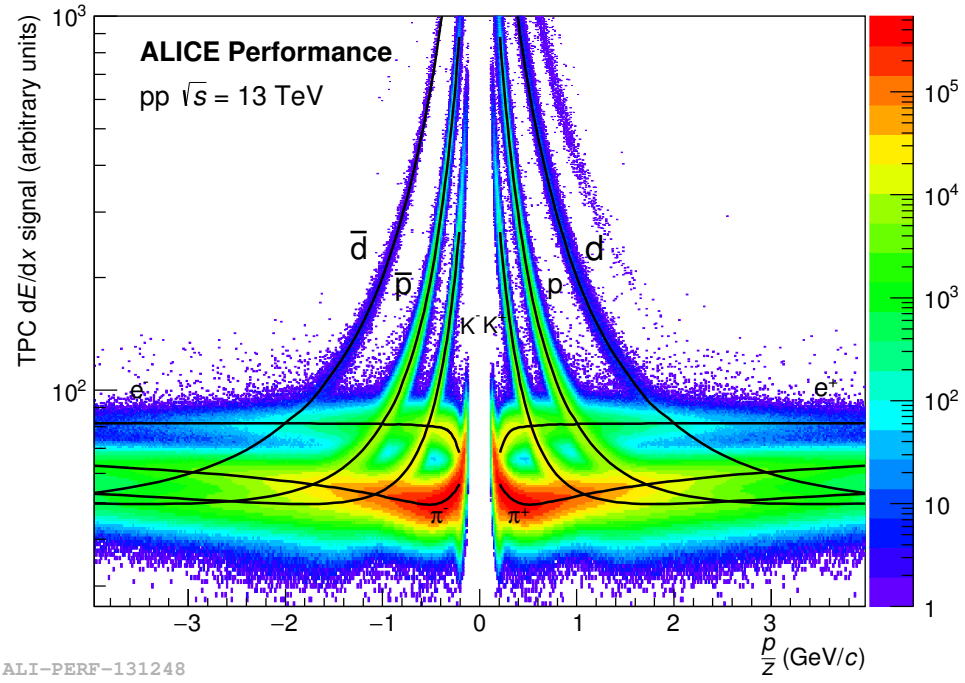

Fig. 1.4: The ionisation energy loss measured in the Time Projection Chamber of ALICE at the Large Hadron Collider (LHC) as a function of the rigidity of particles.

Figure 1.4 shows the ionisation energy loss measured by the biggest TPC ever built and functioned in a high energy experiment, the ALICE (A Large Ion Collider Experiment) at the Large Hadron Collider (LHC) at CERN. The value of dE/dx is measured as a function of the rigidity, defined by the momentum of each particle over the atomic number. One can clearly see the different bands corresponding to different particle species that interact with the gas of the TPC and are reconstructed and at a later stage identified by the TPC.

1.1.1.2 Solid state detectors

When a charged particle traverses an appropriately doped silicon wafer, electron-hole pairs are created by the ionisation process. If a potential difference is applied across the silicon, the holes will drift in the direction of the electric field where they can be collected by the p–n junctions. The sensors can be shaped into silicon strips, typically separated by ≈ 25 μm or into silicon pixels giving a precise two–dimensional space point.

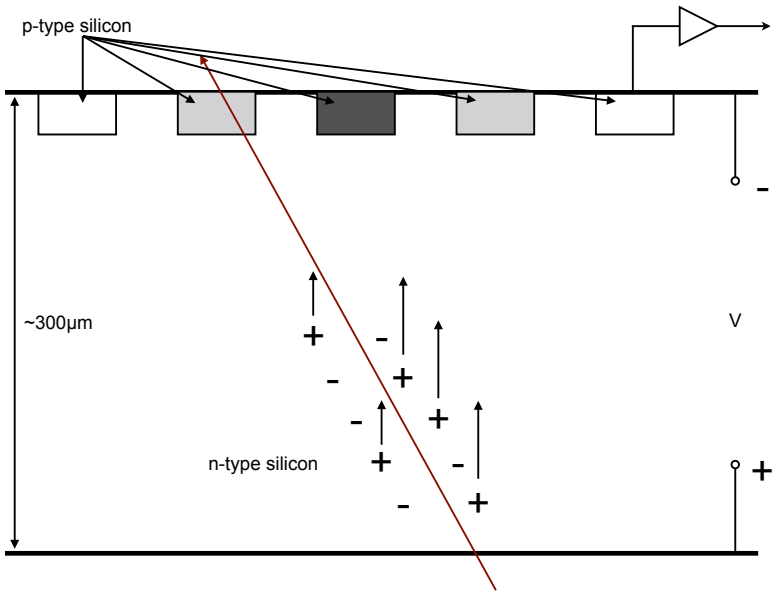

Fig. 1.5: The working principle of a silicon detector.

Silicon tracking detectors typically consist of several layers, cylindrical surfaces of silicon wafers. A schematic view of such configuration is given in fig. 1.6. A charged particle will leave a hit on a silicon sensor in each of the cylindrical layers from where the trajectory of the charged particle track can be reconstructed. The tracking system is usually placed inside a large solenoid producing approximately a uniform magnetic field in the direction of the colliding beams, which is taken to be the z–axis in fig. 1.6. Due to the Lorentz force the trajectory of the particle in the axial magnetic field is a helix with a radius of curvature R and a pitch angle λ. These two variables are connected with the particle's momentum according to

$$p\cos\lambda = 0.3BR,$$

where the momentum p is given in GeV/c, B is the magnetic flux density in T and R is given in meters. By determining the curvature and the pitch angle through the measurement of the helical trajectory, the momentum of the particle can be estimated. For high momentum particles the radius of the curvature can be large. As an example the radius of the curvature of a 100 GeV pion in a 4 T magnetic field as the one used by the Compact Muon Solenoid (CMS) detector at CERN is

$R \approx 100$ m. Even if such particle tracks seem quite straight this small deflection is efficiently detected and measured using precise space points from silicon strip detectors.

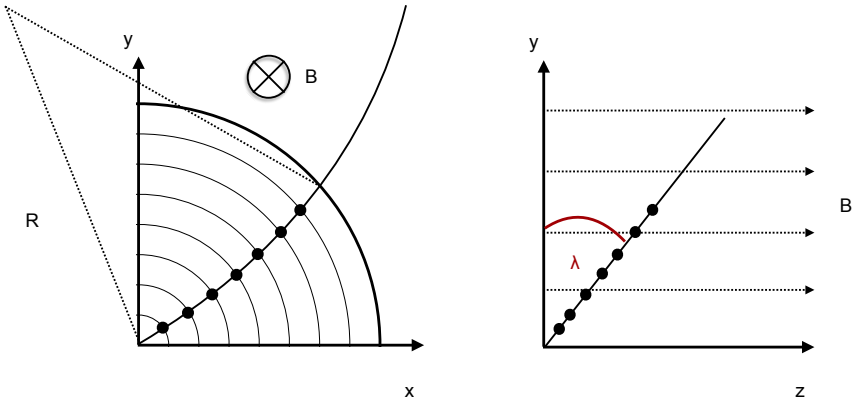

Fig. 1.6: Charged particle track reconstruction from the space points observed in a seven-layer tracking detector. The curvature in the x–y plane (left plot) determines the transverse momentum of the track.

1.1.1.3 Scintillators

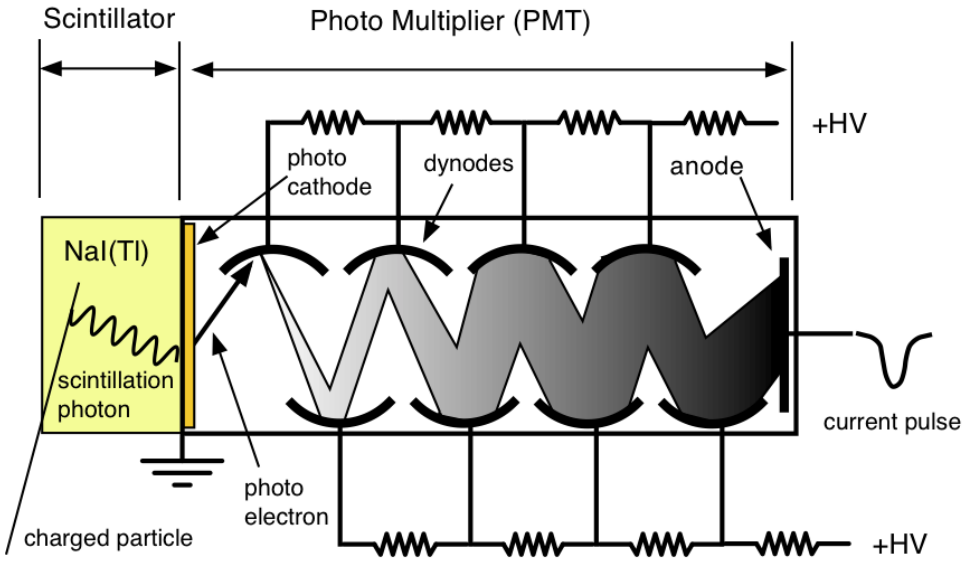

Fig. 1.7: The working principle of a scintillator detector.

A scintillation detector or scintillation counter is obtained when a scintillator is coupled to an electronic light sensor such as a photomultiplier tube (PMT), photodiode, or silicon photomultiplier. PMTs absorb the light emitted by the scintillator and re-emit it in the form of electrons via the photoelectric effect. The subsequent multiplication of those electrons (sometimes called photo-electrons) results in an electrical pulse which can then be analysed and yield meaningful information about the particle that originally struck the scintillator. Vacuum photodiodes are similar but do not amplify the signal while silicon photodiodes, on the other hand, detect incoming photons by the excitation of charge carriers directly in the silicon. Silicon photomultipliers consist of an array of photodiodes which are reverse-biased with sufficient voltage to operate in avalanche mode, enabling each pixel of the array to be sensitive to single photons. Figure 1.7 gives schematically the working principle of an experimental setup utilising a scintillator detector which is coupled to a PMT.

1.1.1.4 Cherenkov radiation

Cherenkov radiation is electromagnetic radiation emitted when a charged particle passes through a dielectric medium at a speed greater than the phase velocity of light in that medium. The characteristic blue glow of an underwater nuclear reactor is due to Cherenkov radiation. It is named after Soviet scientist Pavel Cherenkov, the 1958 Nobel Prize winner who was the first to detect it experimentally.

While electrodynamics holds that the speed of light in a vacuum is a universal constant, the speed at which light propagates in a material may be significantly less than c. For example, the speed of the propagation of light in water is only 0.75 c. Matter can be accelerated beyond this speed (although still to less than c) during nuclear reactions and in particle accelerators. Cherenkov radiation results when a charged particle, most commonly an electron, travels through a dielectric (electrically polarizable) medium with a speed greater than that at which light propagates in the same medium.

Moreover, the velocity that must be exceeded is the phase velocity of light rather than the group velocity of light. The phase velocity can be altered dramatically by employing a periodic medium, and in that case one can even achieve Cherenkov radiation with no minimum particle velocity, a phenomenon known as the Smith?Purcell effect. In a more complex periodic medium, such as a photonic crystal, one can also obtain a variety of other anomalous Cherenkov effects, such as radiation in a backwards direction (whereas ordinary Cherenkov radiation forms an acute angle with the particle velocity). The geometry of the Cherenkov radiation (shown for the ideal case of no dispersion).

As a charged particle travels, it disrupts the local electromagnetic field in its medium. In particular, the medium becomes electrically polarized by the particle's electric field. If the particle travels slowly then the disturbance elastically relaxes back to mechanical equilibrium as the particle passes. When the particle is traveling fast enough, however, the limited response speed of the medium means that a disturbance is left in the wake of the particle, and the energy contained in this disturbance radiates as a coherent shockwave.

A common analogy is the sonic boom of a supersonic aircraft or bullet. The sound waves generated by the supersonic body propagate at the speed of sound itself; as such, the waves travel slower than the speeding object and cannot propagate forward from the body, instead forming a shock front. In a similar way, a charged particle can generate a light shock wave as it travels through an insulator.

Figure 1.8 gives the working principle of the effect of Cherenkov radiation. A particle, represented by the red arrow, travels in a medium with speed v_p such that $c/n < v_p < c$, where c is the speed of light in vacuum, and n is the refractive index of the medium. As an example, if the medium is water, with $n = 1.33$ at $T = 20^o$C, then the condition is $0.75c < v_p < c$. Let us we denote with β the ratio between the speed of the particle and the speed of light i.e. $\beta = v_p/c$. The emitted light waves (blue arrows) travel at speed $v_{em} = c/n$. The left corner of the triangle represents the location of the superluminal particle at some initial moment ($t = 0$). The right corner of the triangle is the location of the particle at some later time t. In the given time t, the particle travels the distance

$$x_p = v_p t = \beta c t$$

whereas the emitted electromagnetic waves are constricted to travel the distance

$$x_{em} = v_{em} t = \frac{c}{n} t$$

The angle θ is then given by:

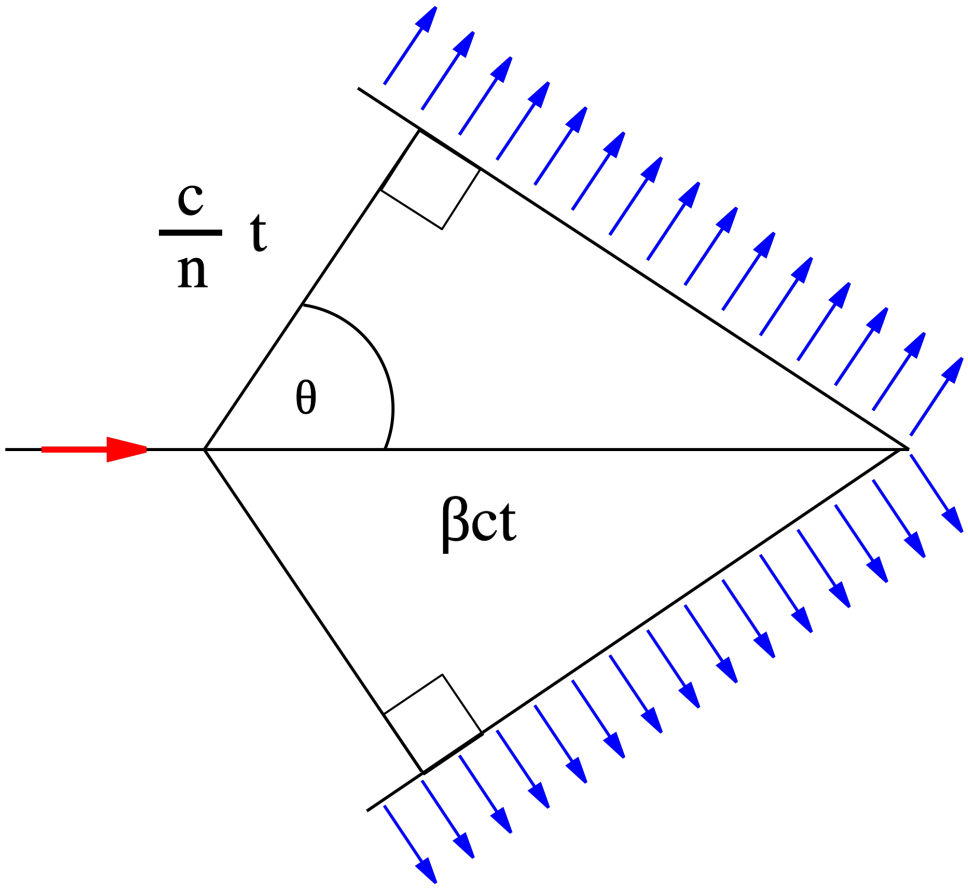

Fig. 1.8: The working principle of the effect of Cherenkov radiation.

$$\cos\theta = \frac{1}{n\beta}$$

Note that since this ratio is independent of time, one can take arbitrary times and achieve similar triangles. The angle stays the same, meaning that subsequent waves generated between the initial time $t = 0$ and final time t will form similar triangles with coinciding right endpoints to the one shown.

Cherenkov radiation is commonly used in experimental particle physics for particle identification. One could measure the velocity of an electrically charged elementary particle by the properties of the Cherenkov light it emits in a certain medium. If the momentum of the particle is measured independently, one could compute the mass of the particle by its momentum and velocity and hence identify the particle.

The simplest type of particle identification device based on a Cherenkov radiation technique is the threshold counter, which gives an answer as to whether the velocity of a charged particle is lower or higher than a certain value ($v_0 = c/n$), by looking at whether this particle does or does not emit Cherenkov light in a certain medium. This threshold behaviour can be utilised to identify particles of a given momentum p. In particular, for a relativistic particle $\beta = pc/E = p/(p^2 + m^2c^2)^{1/2}$ and therefore only particles with mass

$$mc < \sqrt{n^2 - 1}\,p,$$

will produce Cherenkov radiation. Figure 1.9 presents the identification capabilities of a ring-imaging Cherenkov detector used by the ALICE experiment at the LHC.

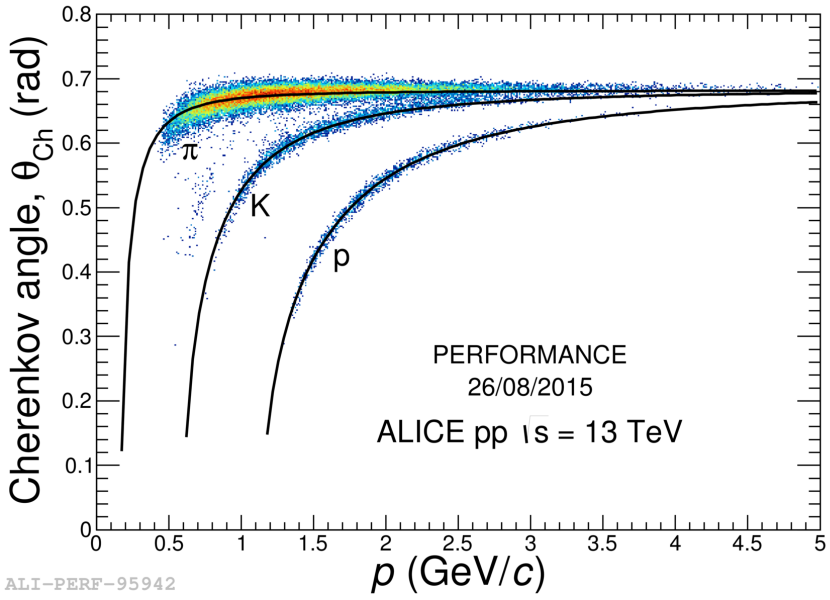

Fig. 1.9: Identifying particles in pp collisions at the LHC using a ring-imaging Cherenkov detecor.

1.1.1.5 Transition radiation detectors

Transition radiation (TR) is a form of electromagnetic radiation emitted when a charged particle passes through inhomogeneous media, such as a boundary between two different media. This is in contrast to Cherenkov radiation, which occurs when a charged particle passes through a homogeneous dielectric medium at a speed greater than the phase velocity of electromagnetic waves in that medium.

Optical transition radiation is produced by relativistic charged particles when they cross the interface of two media of different dielectric constants. The emitted radiation is the homogeneous difference between the two inhomogeneous solutions of Maxwell's equations of the electric and magnetic fields of the moving particle in each medium separately. In other words, since the electric field of the particle is different in each medium, the particle has to "shake off" the difference when it crosses the boundary. The total energy loss of a charged particle on the transition depends on its Lorentz factor $\gamma = E/mc^2$ and is mostly directed forward, peaking at an angle of the order of $1/\gamma$ relative to the particle's path. The intensity of the emitted radiation is roughly proportional to the particle's energy E.

Optical transition radiation is emitted both in the forward direction and reflected by the interface surface. In case of a foil having an angle at 45 degrees with respect to a particle beam, the particle beam's shape can be visually seen at an angle of 90 degrees. More elaborate analysis of the emitted visual radiation may allow for the determination of γ and emittance.

In the approximation of relativistic motion ($\gamma \gg 1$), small angles ($\theta \ll 1$) and high frequency ($\omega \gg \omega_p$), the energy spectrum can be expressed as:

$$\frac{dI}{d\nu} \approx \frac{z^2 e^2 \gamma \omega_p}{\pi c}\left((1+2\nu^2)\ln(1+\frac{1}{\nu^2})-2\right),$$

where z is the atomic charge, e is the charge of an electron, γ is the Lorentz factor, ω_p is the Plasma Frequency. This divergences at low frequencies where the approximations fail. The total energy emitted is:

$$I = \frac{z^2 e^2 \gamma \omega_p}{3c}$$

The characteristics of this electromagnetic radiation makes it suitable for particle discrimination, particularly of electrons and hadrons in the momentum range between 1 GeV/c and 100 GeV/c. The transition radiation photons produced by

electrons have wavelengths in the X–ray range, with energies typically in the range from 5 to 15 keV. However, the number of produced photons per interface crossing is very small: for particles with $\gamma = 2 \times 10^3$, about 0.8 X-ray photons are detected. Usually several layers of alternating materials or composites are used to collect enough transition radiation photons for an adequate measurement.

1.2 Interactions and detection of electrons and photons

At low energies the energy loss of electrons is dominated by ionisation. However, for energies above a critical energy E_{cr}, the main energy loss mechanism is bremsstrahlung where the electron radiates a photon in the presence of the electrostatic field of a nucleus. The critical energy is related to the charge Z of the nucleus and is given by

$$E_{cr} \approx \frac{800}{Z} \text{ MeV}$$

The electrons of interest in the majority of the modern particle physics experiments have an energy at the multi–GeV scale, significantly larger than the critical energy. They therefore interact with matter primarily through bremsstrahlung. The bremsstrahlung effect can occur for all charged particles but the rate is inversely proportional to the square of the mass of the particle. Hence for muons the rate of energy loss through bremsstrahlung is suppressed compared to electrons by a factor of $(m_e/mu_\mu)^2$. This explains why bremsstrahlung is the dominant energy loss mechanism for electrons while for muons ionisation energy loss is still the main energy loss effect (at least for $E_\mu < 100$ GeV).

Photons, at low energies, interact with matter primarily via the photoelectric effect. In this process a photon is absorbed by an atomic electron that is ejected from the atom. At higher energies, $E_\gamma \approx 1$ MeV, the Compton scattering process $\gamma e^- \rightarrow \gamma e^-$ becomes significant. For even higher energies, for $E_\gamma > 10$ MeV, the interactions of photons are dominated by electron–positron pair production in the presence of the field of a nucleus.

The electromagnetic interactions of high energy electrons and photons in matter is characterised by the radiation length X_0. The radiation length is the average distance over which the energy of an electron is reduced by bremsstrahlung by a factor of $1/e$. It is approximately $7/9$ of the mean free path of the e^+e^- pair production for a high–energy photon. The radiation length is related to the atomic number Z of the material and can be approximated by the expression

$$X_0 = \frac{1}{4\alpha n Z^2 r_e^2 ln(287/Z^{1/2})},$$

where n is the number density of nuclei and r_e is the classical radius of the electron, given by

$$r_e = \frac{e^2}{4\pi\varepsilon_0 m_e c^2} = 2.8 \times 10^{-15} \text{ m}$$

For high–Z materials the radiation length is relatively short. As an example $X_0(\text{Fe}) = 1.76$ cm and $X_0(\text{Pb}) = 0.56$ cm.

1.2.1 Electromagnetic showers

When a high–energy electron interacts with mater in a medium it radiates a bremsstrahlung photon which in turns produces an electron–positron pair. The process of bremsstrahlung and pair production continues to produce a cascade of photons, electrons and positrons. This whole process is referred to as electromagnetic shower and an example is given schematically in fig. 1.10. Similarly a high–energy photon will create an electron–positron pair that will in turns produce an electromagnetic shower.

The number of particles in an electromagnetic shower approximately doubles after every radiation length of material traversed. Hence in an electromagnetic shower produced by an electron or photon of energy E, the average energy of particles after x radiation lengths is given by

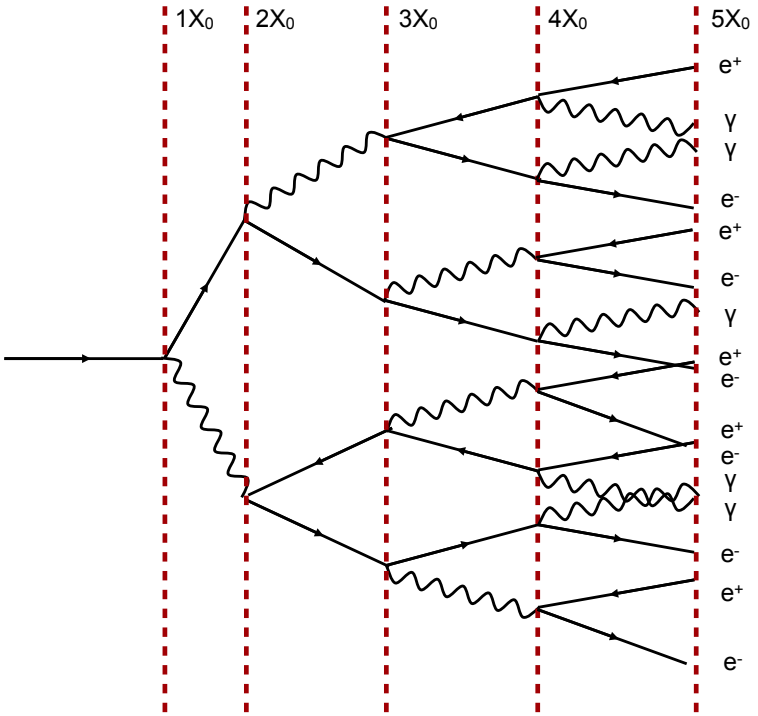

Fig. 1.10: Identifying particles in pp collisions at the LHC using a ring-imaging Cherenkov detector.

$$\langle E \rangle = \frac{E}{2^x}$$

The shower continues to develop until the average energy of the particles falls below the critical energy E_{cr} at which point the electrons and positrons in the cascade loose energy primarily through ionisation. The electromagnetic shower has thus the maximum number of particles after X_{max} radiation lengths given by the condition $\langle E \rangle = E_{cr}$. This point is reached after

$$X_{max} = \frac{ln(E/E_{cr})}{ln2}$$

In a high–Z material such as lead with $E_{cr} \approx 10$ MeV, a 100 GeV electromagnetic shower reaches its maximum at $\approx 13X_0$. This corresponds to about 10 cm of lead. Consequently electromagnetic showers deposit most of their energy in a relatively small region of space.

1.2.2 Electromagnetic calorimeters

In high–energy particle physics experiments the energies of electrons and photons are measured using electromagnetic calorimeters constructed from high–Z material. A popular choice is the usage of lead tungstate ($PbWO_4$) crystals which is an inorganic scintillator. These crystals are both optically transparent and have a short radiation length of $X_0 = 0.83$ cm, allowing the electromagnetic shower to be contained in a compact region. The electrons in the electromagnetic shower produce scintillation light that can be collected and amplified by efficient photon detectors. The amount of scintillation light produced is proportional to the total energy of the original electron or photon. Alternatively, electromagnetic calorimeters can be constructed by alternating layers of high–Z material, such as lead, with an active layer in which the ionisation from the electrons in the electromagnetic shower can be measured. For the electromagnetic calorimeters in large, modern particle physics detectors, the energy resolution for electrons and photons is typically in the range

$$\frac{\sigma_E}{E} \approx \frac{3\% - 10\%}{\sqrt{E/\mathrm{GeV}}}$$

1.3 Interactions and detection of hadrons

Charged hadrons lose energy continuously through ionisation when they interact with matter. In addition, both charged and neutral hadrons can undergo strong interactions with the nuclei of the medium. Particle produced in this primary hadronic interaction will subsequently interact further downstream in the medium, giving rise to a cascade of particles of hadronic, this time, nature. The development of hadronic showers is characterised by the nuclear interaction length, λ_f, defined as the mean distance between hadronic interactions of relativistic hadrons. The nuclear interaction length is significantly larger than the radiation length. As an example, the interaction length for Fe is $\lambda_f(\mathrm{Fe}) \approx 17$ cm, compared to its radiation length of 1.8 cm.

Unlike electromagnetic showers which develop in a uniform manner, hadronic showers are more variable because of the many different final stets that can be produced in high–energy hadronic interactions. In addition, any π^0 produced in the hadronic shower decays almost instantaneously through the channel $\pi \to \gamma\gamma$, leading to an electromagnetic component of the shower. The fraction of the energy in this electromagnetic component depends on the number of π^0s produced and varies from shower to shower. Finally, not all of the energy in a hadronic shower is detectable. On average, around 30% of the incident energy is effectively lost in the form of nuclear excitation and break–up.

1.3.1 Hadronic calorimeters

In particle detector systems the energies of such hadronic showers are measured in a hadron calorimeter. Because of the relatively large distance between nuclear interactions, hadronic showers will occupy a significant volume in any detector. For example, in a typical hadron calorimeter, the shower of a 100 GeV hadron has longitudinal and lateral extents of the order of 2 m and 0.5 m, respectively. A number of different technologies have been used to construct hadron calorimeters. A commonly used technique is to use a sandwich structure of thick layers of high–density absorber material, where the shower develops, and thin layers of active material where the energy deposition from the charged particle in the shower are sampled. Fluctuations in the electromagnetic fraction of the shower and the amount of energy lost in nuclear break–up limits the precision to which the energy can be measured. A typical value for the energy resolution of a hadronic calorimeter is given by

$$\frac{\sigma_E}{E} \geq \frac{50\%}{\sqrt{E/\mathrm{GeV}}}$$

1.4 Setup of modern particle physics experiments

Based on what was described before, a modern particle physics experiment should have the possibility to reconstruct and identify hadrons, measure the energy of highly energetic electrons and photons, estimate the energy deposited by highly energetic hadrons and reconstruct and identify muons. Following these requirements, the basic structure of a modern particle physics experiment is given in fig. 1.11. The experiment typically consists of a cylindrical barrel with its axis parallel to the beam pipe. This cylindrical structure is closed at the two ends with two flat end–caps, thus providing full solid angle coverage, almost down to the beam pipe. The inner region of the experiment is devoted to tracking and identifying charged particles with suitable tracking detectors e.g. based on semi-conductor technology (silicon detectors) or gaseous volumes (TPC). The tracking volume is usually surrounded by an electromagnetic calorimeter that allows to detect electrons and photons. This is followed by a large volume hadronic calorimeter, capable of detecting and measuring

the energy of highly energetic hadrons. Finally, there are dedicated detectors positioned further outwards, devoted to the detection of muons that, as neutrinos, are able to go through the electromagnetic and hadronic calorimeters.

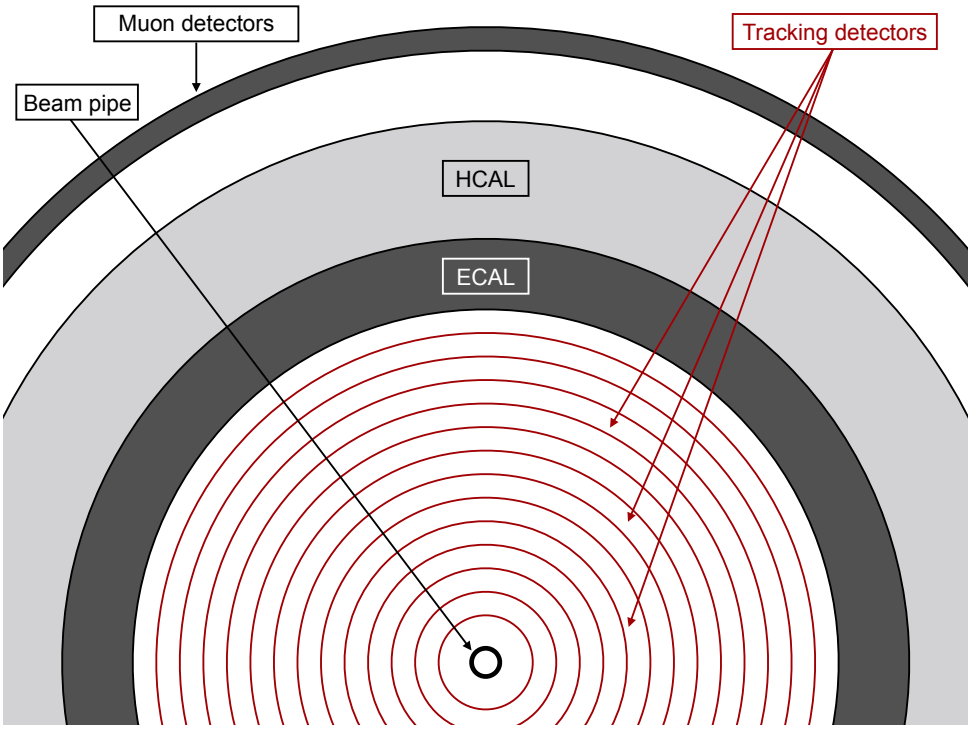

Fig. 1.11: A transverse slice of a typical modern particle physics experiment.

To measure the momentum of particles, as discussed before, a suitable (usually solenoid) magnetic fields is applied inside this barrel region. Different particle species can be detected and identified using one or a combination of techniques discussed in previous paragraphs:

- Information about momentum of charged particles is deduced from the measurement of the curvature of the particle track inside the magnetic field.
- Electrons are identified as charged–particle tracks that leave hits in the tracking detectors and subsequently initiate an electromagnetic shower in the electromagnetic calorimeter.
- Neutral particles are either reconstructed in the tracking detectors (e.g. decays) or their energy is measured in the calorimeters.

  - Neutral particles that decay are reconstructed via their decay topology in the tracking detectors in combination with information from the calorimeters about their decay products (depending on the nature of the decay)

  - Photons are identified in the electromagnetic calorimeter as sources of isolated showers.

  - On the other hand, neutral hadrons will interact with the material in the hadronic calorimeter and initiate an isolated hadronic shower.
- Charged hadrons will be reconstructed from their hits in the tracking detectors, followed by the combination of a small energy deposition via ionisation energy loss in the electromagnetic calorimeter and a large energy deposition in the hadronic calorimeter.
- Finally, special detectors outside the calorimeters are sensitive to the passage of muon tracks, in combination with hits in the tracking detectors and very small energy deposition in both the electromagnetic and the hadronic calorimeters.

One of the last pieces of the puzzle is the detection of neutrinos. Neutrinos, as we have seen, barely interact with matter. However they are carriers of important information and thus need to be accounted for. Their presence in modern particle

physics experiments, whose purpose is not solely the detection of neutrinos, is through the presence of missing momentum, defined as:

$$\mathbf{p}_{missing} = -\sum_i \mathbf{p}_i,$$

where the sum extends over all measured momenta of all observed particles in all directions of an event. If all particles produced in the collision are detected, this sum should be zero provided that the collisions take place in the centre–of–mass frame. Any significant deviation from zero indicates the presence of energetic neutrinos in the event.

1.5 Measurements at particle accelerators

If one excludes the studies related to properties of neutrinos and the discovery of gravitational waves (not directly particle physics related topic), the major breakthroughs in particle physics have come from experiments at high–energy particle accelerators. Particle accelerators can be divided in two categories:

- colliding beams machines where two beams of particles are accelerated at high velocities, circulate in opposite directions and are brought to collision,
- fixed–target experiments where a single beam is accelerated at high velocities and collides into a stationary target.

The production and eventual discovery of massive particles, such as the carriers of the weak force Z^0 and $W^{\pm}$, or even the Higgs boson discovered in 2012 at CERN requires that the energy available in such collisions in the centre–of–mass frame is greater than the sum of masses of the final state particles. The centre–of–mass energy, as we saw in previous chapters, is a Lorentz invariant quantity and is given by

$$s = \sqrt{\mathbf{P}_{i\mu}\mathbf{P}_i^{\mu}} = \sqrt{\left(\sum_i E_i\right)^2 - \left(\sum_i p_i\right)^2} \tag{1.5.1}$$

In a fixed target experiment, momentum conservation implies that the final state particles are always produced with significant kinetic energy and they are produced mainly in the so–called forward region. The corresponding centre–of–mass energy is given by:

$$s = (E_{\text{beam}} + M_{\text{target}})^2 - p_{\text{beam}}^2 = M_{beam}^2 + M_{\text{target}}^2 + 2M_{\text{target}}E_{\text{beam}} \tag{1.5.2}$$

where E_{beam}, p_{beam} and M_{beam} are the energy, momentum and mass of the beam particles respectively, while M_{target} is the mass of the target particle. Colliding beam machines have the advantage of achieving much higher centre–of–mass energy than fixed target configurations.

Only stable charged particles can be accelerated to high energies, thus limiting the possibilities for colliding configurations to e^+e^- colliders, hadron colliders (e.g. pp, $\text{p}\overline{\text{p}}$, e^+p or e^-p colliders and finally heavy–ion colliders. Table **??** presents the basic parameters of recent particle accelerators.

Collider	Laboratory	Colliding system	Data of operation	$\sqrt{s}$/GeV	Luminosity/cm^{-2}s^{-1}
PEP–B	SLAC	e^+e^-	1999–2008	10.5	1.2×10^{34}
KEKB	KEK	e^+e^-	1999–2010	10.6	12.1×10^{34}
LEP	CERN	e^+e^-	1989–2000	90–209	10^{32}
HERA	DESY	e^+p/e^-p	1992–2007	320	8×10^{31}
Tevatron	Fermilab	$\text{p}\overline{\text{p}}$	1987–2002	1960	4×10^{32}
LHC	CERN	pp/pPb/PbPb	2009–today	14000/5000/5000	10^{34} (for pp)

Table 1.1: The basic parameters of the recent particle accelerators.

Two of the most important parameters of these accelerators are the centre–of–mass energy that gives an idea of the physics reach of each machine but also the luminosity L which determines the rate of events. For a given process the number of interactions is the product of the luminosity integrated over the lifetime of the operation of the machine and the cross-section σ of the process in question:

$$N = \sigma \int L(t)dt$$

The cross-section is a measure of the probability for a given interaction to occur. In order to convert the observed number of events of a particular type into the cross-section of a given process, the integrated luminosity needs to be estimated. Typically the particles in an accelerator are grouped in bunches that are brought into collisions at one or more interaction points. As an example, at the LHC the bunches are separated by 25 ns corresponding to a collision frequency of $f = 40$ MHz. The instantaneous luminosity of the machine can be expressed in terms of the number of particles in the colliding bunches, n_1 and n_2, the frequency at which the bunches collide, and the root–mean–square (rms) of the horizontal and vertical beam sizes, σ_x and σ_y. Assuming that the beams have a Gaussian profile and collide head–on, the instantaneous luminosity is given by

$$L = f \frac{n_1 n_2}{4\pi\sigma_x\sigma_y} \tag{1.5.3}$$